

# We are IntechOpen, the world's leading publisher of Open Access books Built by scientists, for scientists

6,900

Open access books available

186,000

International authors and editors

200M

Downloads

Our authors are among the

154

Countries delivered to

TOP 1%

most cited scientists

12.2%

Contributors from top 500 universities



WEB OF SCIENCE™

Selection of our books indexed in the Book Citation Index  
in Web of Science™ Core Collection (BKCI)

Interested in publishing with us?  
Contact [book.department@intechopen.com](mailto:book.department@intechopen.com)

Numbers displayed above are based on latest data collected.  
For more information visit [www.intechopen.com](http://www.intechopen.com)



---

# Optical Coherence Tomography for Coronary Artery Plaques – A Comparison with Intravascular Ultrasound

---

Kawasaki Masanori

Additional information is available at the end of the chapter

<http://dx.doi.org/10.5772/53955>

---

## 1. Introduction

In an angioscopic study, Mizuno et al. demonstrated that disruption or erosion of vulnerable plaques and subsequent thromboses are the most frequent cause of acute coronary syndrome (Mizuno et al., 1992). A pathological study by Horie et al. demonstrated that plaque rupture into the lumen of a coronary artery may precede and cause thrombus formation leading to acute myocardial infarction (Horie et al., 1978). The stability of atherosclerotic plaques is related to the histological composition of plaques and the thickness of fibrous caps. Therefore, recognition of the tissue characteristics of coronary plaques is important to understand and prevent acute coronary syndrome. Accurate identification of the tissue characteristics of coronary plaques *in vivo* may allow the identification of vulnerable plaques before the development of acute coronary syndrome.

Recently, intravascular optical coherence tomography (OCT) provides high-resolution, cross-sectional images of tissue *in situ* and has an axial resolution of 10  $\mu\text{m}$  and a lateral resolution of 20  $\mu\text{m}$  (Tearney et al., 1997; Brezinski et al., 1996). The OCT images of human coronary atherosclerotic plaques obtained *in vivo* provide additional, more detailed structural information than intravascular ultrasound (IVUS) (Jang et al., 2002; Jang et al., 2005; Kume et al. 2005). Characterizing different types of atherosclerotic plaques on the basis of sensitivity and specificity compared to histological findings to determine plaque vulnerability was established in a previous study (Yabushita et al., 2002). According to this study, the sensitivity and specificity of the classification of the plaque components were sufficient for tissue characterization in clinical settings.

In the 1990's, a new technique was developed that could characterize myocardial tissues by integrated backscatter (IB) analysis of ultrasound images. This technique is capable of providing both conventional two-dimensional echocardiographic images and IB images. Ultra-

sound backscatter power is proportional to the difference of acoustic characteristic impedance that is determined by the density of tissue multiplied by the speed of sound. In studies of the myocardium, calibrated myocardial IB values were significantly correlated with the relative volume of interstitial fibrosis (Picano, 1990 et al.; Naito et al., 1996). In preliminary studies in vitro, IB values reflected the structural and biochemical composition of atherosclerotic lesion and could differentiate fibrofatty, fatty and calcification of arterial walls (Barziliai et al., 1987; Urbani et al., 1993; Picano et al., 1988). It was also reported that anisotropy of the direction and backscatter power is related to plaque type (De Kroon et al., 1991). Takiuchi et al. found that quantitative tissue characterization using IB ultrasound could identify lipid pool and fibrosis in human carotid and/or femoral arteries (Takiuchi et al., 2000). In the early 2000s, it was reported that IB values measured in vivo in human carotid arteries correlated well with postmortem histological classification (Kawasaki et al., 2001). This new non-invasive technique using IB values could characterize the two-dimensional structures of arterial plaques in vivo. With this technique, plaque tissues were classified based on histopathology into 6 types, i.e. intraplaque hemorrhage, lipid pool, intimal hyperplasia, fibrosis, dense fibrosis, and calcification. This technique was applied in the clinical setting to predict cerebral ischemic lesions after carotid artery stenting. From the analysis of receiver operating characteristic (ROC) curves, a relative intraplaque hemorrhage + lipid pool area of 50% measured by IB ultrasound imaging was the most reliable cutoff value for predicting cerebral ischemic lesions evaluated by diffusion-weighted magnetic resonance imaging after carotid artery stenting (Yamada et al., 2010).

In the next generation, this ultrasound IB technique was applied to coronary arteries by use of intravascular ultrasound (IVUS) (Kawasaki et al., 2010). In the IVUS analysis, 512 vector lines of ultrasound signal around the circumference were analyzed to calculate the IB values. The IB values for each tissue component were calculated using a fast Fourier transform, and expressed as the average power, measured in decibels (dB), of the frequency component of the backscattered signal from a small volume of tissue.

## **2. Comparison among OCT, IB-IVUS and conventional IVUS for tissue characterization of coronary plaques**

Before OCT and IVUS imaging, arteries were warmed to 37 °C in saline. Coronary arteries were imaged with 3.2 F OCT catheters. The position of the interrogating beam on the tissue was monitored by a visible light beam (laser diode, 635 nm) that was coincident with the infrared beam. A total of 128 regions of interest (ROI 0.2 × 0.2 mm) on the OCT images and classified tissue characteristics in the ROIs according to the definitions described in a previous study (Jang et al., 2002). All OCT diagnoses were performed by two skilled readers blinded to the diagnoses based on IVUS and histology. For the comparison with diagnoses based on histology, ROIs from the OCT images in which the diagnoses made by the two OCT readers were identical were used. Conventional IVUS images and IB signals were acquired using an IVUS system (Clear View, Boston Scientific, Natick, Massachusetts) and a 40 MHz intravascular catheter. Definitions of IB values for each histological category were de-

terminated by comparing the histological images as reported in a previous study (Kawasaki et al., 2002). To clarify the rotational and cross-sectional position of the included segment, multiple surgical needles were carefully inserted into the coronary arteries before OCT and IVUS imaging to serve as reference points to compare the imaging modalities.

The overall agreement between the OCT and the histological diagnoses was excellent (Cohen’s  $\kappa = 0.92$ , 95% CI: 0.85 - 1.00). The overall agreement between the IB-IVUS and histological diagnoses was 0.80 (95% CI: 0.69 - 0.92). The overall agreement of between the conventional IVUS and histological diagnoses was 0.59 (95% CI: 0.42 - 0.77) (Table 1). The overall agreement between the OCT and the IB-IVUS diagnoses was 0.77 (95% CI: 0.65 - 0.90). The overall agreement between the OCT and conventional IVUS diagnoses was 0.62 (95% CI: 0.44 - 0.79) (Table 5). False-positive diagnoses of IB-IVUS and conventional IVUS for lipid pool often contained histological evidence of small amounts of lipid accumulation within a predominantly fibrous lesion. These lesions that included a clinically irrelevant amount of lipid pool were identified as lipid pool by IB-IVUS ( $n = 3$ ) and echo-lucent by conventional IVUS ( $n = 5$ ), and reduced the negative predictive values for fibrosis (84% and 74%) (Kawasaki et al., 2006).

|   | Histology |    |    |    | Total |
|---|-----------|----|----|----|-------|
|   | CL        | FI | LP | IH |       |
| <b>OCT</b>  |           |    |    |    |       |
| Calcification   | 7         | 0  | 0  | 0  | 7     |
| Fibrosis  | 0         | 86 | 1  | 1  | 88    |
| Lipid pool  | 0         | 2  | 18 | 0  | 20    |
| Intimal hyperplasia   | 0         | 0  | 0  | 6  | 6     |
| Total   | 7         | 88 | 19 | 7  | 121   |
| Cohen’s $\kappa = 0.92$ (0.85 - 0.99), Weighted $\kappa = 0.92$ (0.85 - 1.00) |           |    |    |    |       |

|   | Histology |    |    |    | Total |
|---|-----------|----|----|----|-------|
|   | CL        | FI | LP | IH |       |
| <b>IB-IVUS</b>  |           |    |    |    |       |
| Calcification   | 7         | 1  | 0  | 0  | 8     |
| Fibrosis  | 0         | 77 | 3  | 2  | 82    |
| Lipid pool  | 0         | 3  | 16 | 0  | 19    |
| Intimal hyperplasia   | 0         | 1  | 0  | 4  | 5     |
| Total   | 7         | 82 | 19 | 6  | 114   |
| Cohen’s $\kappa = 0.80$ (0.69 - 0.92), Weighted $\kappa = 0.79$ (0.66 - 0.92) |           |    |    |    |       |

|                          | Histology |    |    |    | Total |
|--------------------------|-----------|----|----|----|-------|
|                          | CL        | FI | LP | IH |       |
| <b>Conventional IVUS</b> |           |    |    |    |       |
| Calcification            | 7         | 1  | 0  | 0  | 8     |
| Fibrosis                 | 0         | 74 | 5  | 6  | 85    |
| Lipid pool               | 0         | 5  | 10 | 0  | 15    |
| Intimal hyperplasia      | 0         | 0  | 0  | 0  | 0     |
| Total                    | 7         | 80 | 15 | 6  | 108   |

Cohen’s  $\kappa = 0.59$  (0.42 - 0.77), Weighted  $\kappa = 0.54$  (0.35 - 0.72)

CL: calcification, FI: fibrosis, LP: lipid pool, IH: intimal hyperplasia

**Table 1.** Comparison between imaging diagnosis and histological diagnosis

OCT diagnoses, in which two OCT readers diagnoses were identical, were in excellent agreement with the histological diagnoses. False negative and false positive diagnoses for lipid-rich plaque were seen comparing the OCT images and histological findings (Yabushita et al., 2002). However, false negative diagnoses for lipid-rich plaque, which could be attributed to the limited penetration depth of OCT (1.25 - 2 mm), were not seen because all ROIs were set within the penetration depth of OCT. In addition, false positive diagnoses for lipid-rich plaque, which could be attributed to difficulty of differentiating clinically relevant large lipid pools and insignificant lipid accumulation were not seen because of the small ROIs (0.2 mm x 0.2 mm).

### **3. Comparison of the thickness of the fibrous cap measured by OCT and IB-IVUS in vivo**

During routine selective percutaneous coronary intervention in 42 consecutive patients, a total of 28 cross-sections that consisted of lipid overlaid by a fibrous cap were imaged by both IVUS and optical coherence tomography in 24 patients with stable angina pectoris. A 0.016-inch optical coherence tomography catheter (Imagewire, LightLab Imaging, Inc., Westford, MA) was advanced into the coronary arteries. IB-IVUS and optical coherence tomography (M2 OCT Imaging system, LightLab Imaging, Inc., Westford, MA) were performed in each patient at the same site without significant stenosis as described below.

IB-IVUS images were obtained every one second using an automatic pullback device at a rate of 0.5 mm/sec. optical coherence tomography images were obtained using an automatic pullback system at a rate of 0.5 mm/sec. IB-IVUS images were obtained at 0.5 mm intervals, whereas optical coherence tomography images were obtained at 0.03 mm intervals. Therefore, the segments of coronary artery to compare between the two methods were selected based on the IB-IVUS images. Then, these same coronary segments were identified in optical coherence tomography using the distance from easily-definable side branches and calcification as reference markers to ensure that IB-IVUS and optical coherence tomography were compared at the same site. The cross-sections that did not have sufficient imaging quality to analyze tissue characteristics were excluded from the comparison. In the IB-IVUS analysis, images were processed by a smoothing method that averaged nine IB values in nine pixels located in a square field of the color-coded maps to reduce uneven surfaces of tissue components produced by signal noise.

Fibrous caps that overlaid lipid pool were divided into ROI (every 10° rotation from the center of the vessel lumen) and the average thickness was determined. The average thickness of fibrous cap was determined by averaging the thickness of fibrous cap every 2° within the ROIs (Figure 1). The areas where the radial axis from the center of the vessel lumen crossed the tangential line of the vessel surface with an angle less than a 80° were excluded from the comparison.

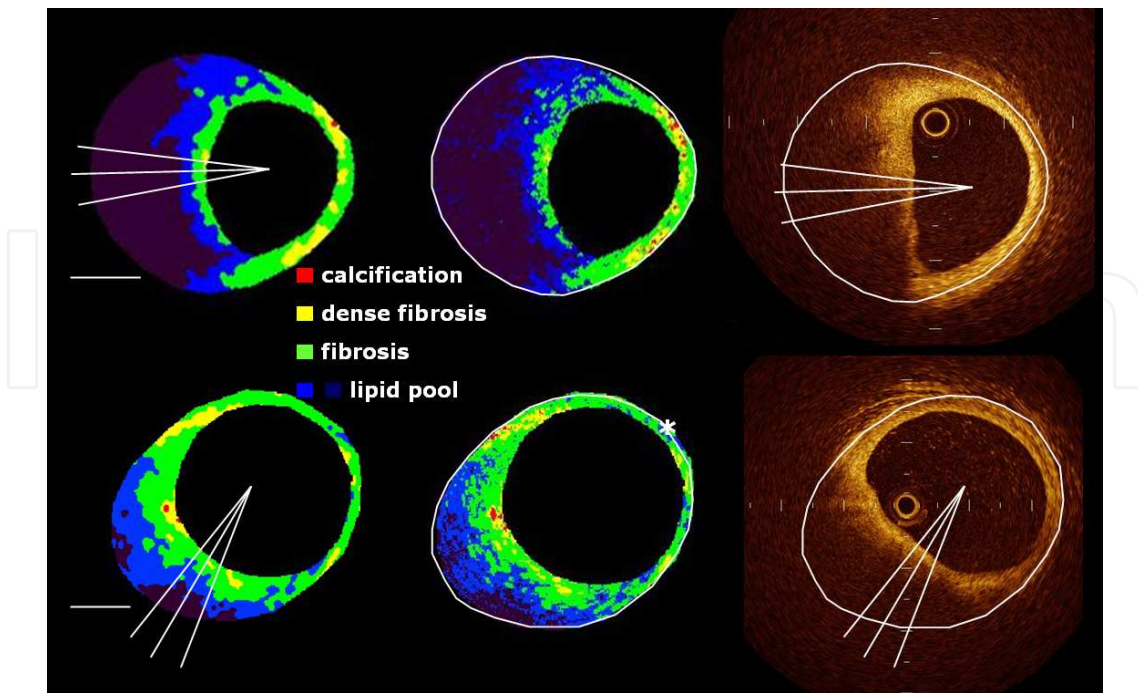


**Figure 1.** Left) Representative integrated backscatter intravascular ultrasound (IB-IVUS) images processed by a smoothing method. (Middle) Original IB-IVUS images (Right) Corresponding optical coherence tomography. \*: attenuation by guide wire. Bar = 1mm.

The thickness of fibrous cap measured by IB-IVUS was significantly correlated with that measured by optical coherence tomography ( $y = 0.99x - 0.19$ ,  $r = 0.74$ ,  $p < 0.001$ ) (Figure 2) (Kawasaki et al., 2010).

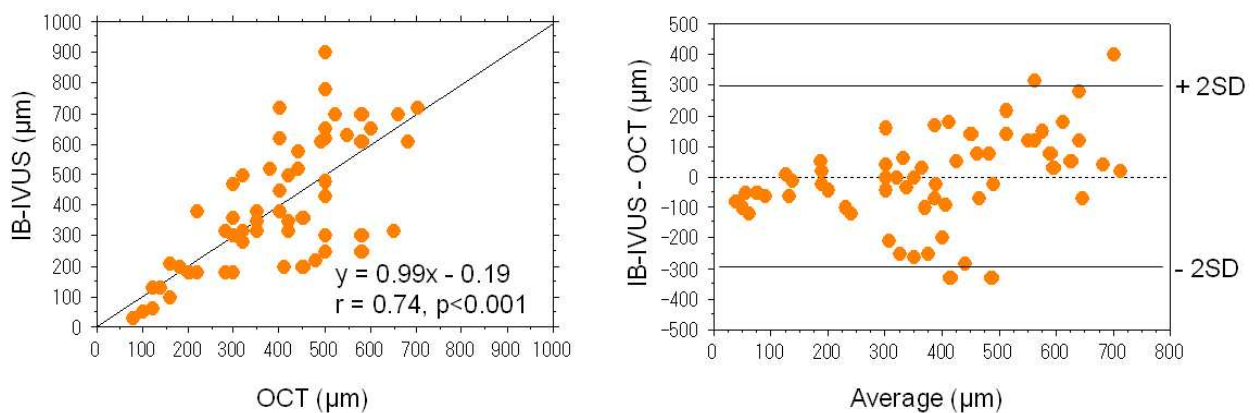


**Figure 2.** Left: Correlation between the thickness of fibrous cap measured by integrated backscatter intravascular ultrasound and optical coherence tomography. Right: Bland-Altman plot.

A Bland-Altman plot showed that the mean difference between the thickness of fibrous cap measured by IB-IVUS and optical coherence tomography (IB-IVUS - optical coherence tomography) was  $-2 \pm 147 \mu\text{m}$  (Figure 2). The difference between the two methods appeared to increase as the thickness of the fibrous cap increased (Figure 3).

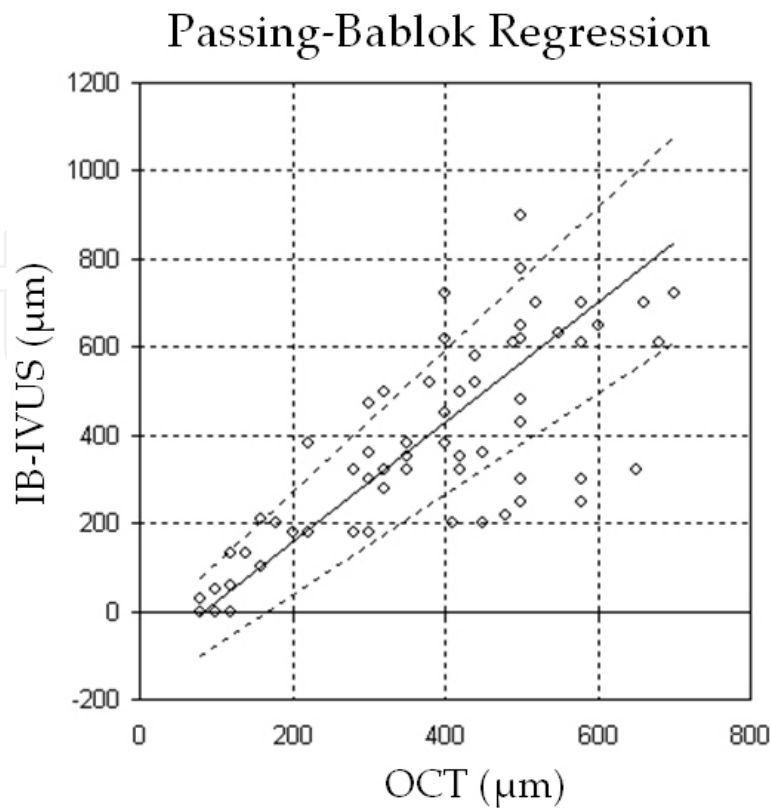


**Figure 3.** Passing-Bablok regression analysis.

Optical coherence tomography has a better potential for characterizing tissue components located on the near side of the vessel lumen, whereas IB-IVUS has a better potential for characterizing tissue components of entire plaques (Kawasaki et al., 2006).

#### 4. Limitations

There were a few limitations of the ultrasound method. First, the angle-dependence of the ultrasound signal makes tissue characterization unstable when lesions are not perpendicular to the ultrasound axis. Picano et al. reported that angular scattering behavior is large in calcified and fibrous tissues, whereas it is slight to nonexistent in normal and fatty plaques (Picano et al., 1985). According to that report, although there was no crossover of IB values between fibrous and fibrofatty within an angle span of  $10^\circ$ , or between fibrous and fatty within an angle span of  $14^\circ$ , this angle-dependence of the ultrasound signal might be partially responsible for the variation of IB values obtained from each tissue component. There was also a report that demonstrated the degree of angle-dependence of 30 MHz ultrasound in detail (Courtney et al., 2002). In that report, the angle-dependence of 30 MHz ultrasound in

the arterial intima and media was 1.11dB/10°. When the 40 MHz catheter was used, the angle dependence increased in arterial tissue. This angle-dependence of the ultrasound signal may decrease the diagnostic accuracy for differentiating tissue components.

Second, the guidewire was not used in the process of imaging because the present studies were performed *ex vivo*. Imaging artifacts *in vivo* due to the guidewire may decrease the diagnostic accuracy. However, removal of the guidewire during imaging after completing the intervention procedure and/or excluding the area behind calcification from the analysis may be necessary in the clinical setting to eliminate this problem. Finally, detecting thrombus from a single IVUS cross-section was not possible because we usually look at multiple IVUS images over time for speckling, scintillation, motion and blood flow in the “microchannel” (Mintz et al., 2001). The analysis of IB values in multiple cross-sections over time is required for the detection of thrombus.

## Author details

Kawasaki Masanori

Address all correspondence to: [masanori@ya2.so-net.ne.jp](mailto:masanori@ya2.so-net.ne.jp)

Department of Cardiology, Gifu University Graduate School of Medicine, Japan

## References

- [1] Barziliai B, Shffitz JE, Miller JG, Sobel BE. (1987). Quantitative ultrasonic characterization of the nature of atherosclerotic plaques in human aorta. *Circ Res.*Vol 60: 459-63.
- [2] Brezinski ME, Tearney GJ, Bouma BE, Izatt JA, Hee MR, Swanson EA, Southern JF, Fujimoto JG. (1996). Optical coherence tomography for optical biopsy: properties and demonstration of vascular pathology. *Circulation* Vol 93:1206–1213.
- [3] Brezinski ME, Tearney GJ, Weissman NJ, Boppart SA, Bouma BE, Hee MR, Weyman AE, Swanson EA, Southern JF, Fujimoto JG. (1997). Assessing atherosclerotic plaque morphology: comparison of optical coherence tomography and high frequency intravascular ultrasound. *Heart* Vol 77:397-403.
- [4] Brown BG, Zhao XQ, Sacco DE, Albers JJ. (1993). Lipid lowering and plaque regression. New insights into prevention of plaque disruption and clinical events in coronary disease. *Circulation.* Vol 87:1781-91.
- [5] Courtney BK, Robertson AL, Maehara A, Luna J, Kitamura K, Morino Y, et al. (2002). Effect of transducer position on backscattered intensity in coronary arteries. *Ultrasound in Med & Biol.* Vol 28:81-91.

- [6] De Kroon MGM, van der Wal LF, Gussenhoven WJ, Rijsterborgh H, Bom N. (1991). Backscatter directivity and integrated backscatter power of arterial tissue. *Int J Card Imaging*. Vol 6:265-75.
- [7] Horie, T., Sekiguchi, M., Hirosawa, K. (1978). Coronary thrombosis in pathogenesis of acute myocardial infarction. Histopathological study of coronary arteries in 108 necropsied cases using serial section. *Br Heart J* Vol. 40:153-61.
- [8] Jang IK, Bouma BE, Kang DH, Park SJ, Park SW, Seung KB, Choi KB, Shishkov M, Schlendorf K, Pomerantsev E, Houser SL, Aretz HT, Tearney GJ. (2002). Visualization of coronary atherosclerotic plaques in patients using optical coherence tomography: comparison with intravascular ultrasound. *J Am Coll Cardiol* Vol 39:604–609.
- [9] Jang IK, Tearney GJ, MacNeill B, Takano M, Moselewski F, Iftima N, Shishkov M, Houser S, Aretz HT, Halpern EF, Bouma BE. (2005). In vivo characterization of coronary atherosclerotic plaque by use of optical coherence tomography. *Circulation* Vol 111:1551-1555.
- [10] Kawasaki M, Takatsu H, Noda T, Ito Y, Kunishima A, Arai M, Nishigaki K, Takemura G, Morita N, Minatoguchi S, Fujiwara H. (2001). Non-invasive tissue characterization of human atherosclerotic lesions in carotid and femoral arteries by ultrasound integrated backscatter. -Comparison between histology and integrated backscatter images before and after death- *J Am Coll Cardiol*. Vol 38:486-92
- [11] Kawasaki M, Takatsu H, Noda T, Sano K, Ito Y, Hayakawa K, Tsuchiya K, Arai M, Nishigaki K, Takemura G, Minatoguchi S, Fujiwara T, Fujiwara H. (2002) In vivo quantitative tissue characterization of human coronary arterial plaques by use of integrated backscatter intravascular ultrasound and comparison with angioscopic findings. *Circulation* Vol 105:2487-2492.
- [12] Kawasaki M, Bouma BE, Bressner J, Houser SL, Nadkarni SK, MacNeill BD, Jang IK, Fujiwara H, Tearney GJ. (2006). Diagnostic accuracy of optical coherence tomography and integrated backscatter intravascular ultrasound images for tissue characterization of human coronary plaques. *J Am Coll Cardiol* Vol 48:81-8.
- [13] Kawasaki M, Hattori A, Ishihara Y, Okubo M, Nishigaki K, Takemura G, Saio M, Takami T, Minatoguchi S. (2010). Tissue characterization of coronary plaques and assessment of thickness of fibrous cap using integrated backscatter intravascular ultrasound. Comparison with histology and optical coherence tomography. *Circ J* Vol 74:2641-48.
- [14] Kume T, Akasaka T, Kawamoto T, Watanabe N, Toyota E, Neishi Y, Sukmawan R, Sadahira Y, Yoshida K. (2005). Assessment of coronary intima-media thickness by optical coherence tomography: comparison with intravascular ultrasound. *Circ J* Vol 69:903-907.
- [15] Mintz GS, Nissen SE, Anderson WD, Bailey SR, Erbel R, Fitzgerald PJ, Pinto FJ, Rosenfield K, Siegel RJ, Tuzcu EM, Yock PG. (2001). American College of Cardiology

- clinical expert consensus document on standards for acquisition, measurement and reporting of intravascular ultrasound studies (IVUS). A report of the American College of Cardiology task force on clinical expert consensus documents developed in collaboration with the European society of cardiology endorsed by the society of cardiac angiography and interventions. *J Am Coll Cardiol*. Vol 37:1478-92.
- [16] Mizuno K, Satomura K, Miyamoto A, Arakawa K, Shibuya T, Arai T, Kurita A, Nakamura H, Ambrose JA. (1992). Angioscopic evaluation of coronary artery thrombi in acute coronary syndromes. *N Engl J Med* Vol 326:287-91.
- [17] Naito J, Masuyama T, Mano T, Kondo H, Yamamoto K, Nagano R, Doi Y, Hori M, Kamada T. (1996). Ultrasound myocardial tissue characterization in the patients with dilated cardiomyopathy: Value in noninvasive assessment of myocardial fibrosis. *Am Heart J*. Vol 131:115-21.
- [18] Picano E, Landini L, Distanto A, Salvadori M, Lattanzi F, Masini M, L'Abbate A. (1985). Angle dependence of ultrasonic backscatter in arterial tissues: a study in vitro. *Circulation*. Vol 72:572-6.
- [19] Picano E, Landini L, Lattanzi F, Salvadori M, Benassi A, L'Abbate A. (1988). Time domain echo pattern evaluation from normal and atherosclerotic arterial walls: a study in vitro. *Circulation*. Vol 77:654-9.
- [20] Picano E, Pelosi G, Marzilli M, Lattanzi F, Benassi A, Landini L, L'Abbate A. (1990). In vivo quantitative ultrasonic evaluation of myocardial fibrosis in humans. *Circulation*. Vol 81:58-64.
- [21] Takiuchi S, Rakugi H, Honda K, Masuyama T, Hirata N, Ito H, Sugimoto K, Yanagitani Y, Moriguchi K, Okamura A, Higaki J, Ogihara T. (2000). Quantitative ultrasonic tissue characterization can identify high-risk atherosclerotic alteration in human carotid arteries. *Circulation* Vol 102:766-70.
- [22] Tearney GJ, Brezinski ME, Bouma BE, Boppart SA, Pitris C, Southern JF, Fujimoto JG. (1997). In vivo endoscopic optical biopsy with optical coherence tomography. *Science* Vol 276:2037–2039.
- [23] Urbani MP, Picano E, Parenti G, Mazzarisi A, Fiori L, Paterni M, Pelosi G, Landini L. (1993). In vivo radiofrequency-based ultrasonic tissue characterization of the atherosclerotic plaque. *Stroke*. Vol 24:1507-12.
- [24] Yabushita H, Bouma BE, Houser SL, Aretz HT, Jang IK, Schlendorf KH, Kauffman CR, Shishkov M, Kang DH, Halpern EF, Tearney GJ. (2002). Characterization of human atherosclerosis by optical coherence tomography. *Circulation* 106:1640-1645.
- [25] Yamada K, Kawasaki M, Yoshimura S, Enomoto Y, Asano T, Minatoguchi S, Iwama T. (2010). Prediction of silent ischemic lesions after carotid artery stenting using integrated backscatter ultrasound and magnetic resonance imaging. *Atherosclerosis* Vol 208:161-6.

